Journal of Physical Science, Vol. 29(3), 95–107, 2018

# Synthesis and Characterisation of Rice Husk Ash Silica Drug Carrier for α-Mangostin

Anwar Iqbal,[1*] Nur Azfa Muhammad Shuib,[2] Deny Susanti Darnis,[2] Mazidatulakmam Miskam,[1] Nur Ruzaina Abdul Rahman[1] and Farook Adam[1]

[1]School of Chemical Sciences, Universiti Sains Malaysia,
11800 USM Pulau Pinang, Malaysia
[2]Department of Chemistry, Kulliyyah of Science, International Islamic University Malaysia, Kuantan Campus, 25200 Kuantan, Pahang, Malaysia
[*]Corresponding author: anwariqbal@usm.my

Published online: 25 November 2018

To cite this article: Iqbal, A. et al. (2018). Synthesis and characterisation of rice husk ash silica drug carrier for α-mangostin. *J. Phys. Sci.*, 29(3), 95–107, https://doi.org/10.21315/jps2018.29.3.8

To link to this article: https://doi.org/10.21315/jps2018.29.3.8

**ABSTRACT:** *The potential of rice husk ash (RHA) silica prepared via sol-gel method (RHA-Si) as a drug carrier was investigated. The nitrogen adsorption-desorption isotherm of RHA-Si indicates the presence of mesopores and some small percentage of micropores. The Brunauer, Emmett and Teller (BET) surface area of RHA-Si was 589 $m^2$ $g^{-1}$ and the Barrett-Joyner-Halenda (BJH) pore size was 5.1 nm. The adsorption of α-mangostin was confirmed by Fourier transform infrared (FTIR) spectroscopy and thermogravimetric analysis (TGA). The sample containing α-mangostin was labeled as RHA-Si-α. The BET surface area of RHA-Si-α was 110 $m^2$ $g^{-1}$ with the BJH pore size of 24.4 nm. The X-ray powder diffraction (XRD) showed that the RHA-Si and RHA-Si-α were amorphous. The disappearance of crystallinity of α-mangostin indicates that the solubility and dissolution of α-mangostin have been improved. The drug release profile indicated a burst release corresponding to 47% of the total drug loading in the first 15 min. The burst release was caused by physically adsorbed drug molecules. The findings suggest that RHA silica has potential application as nano drug carrier.*

**Keyword:** Rice husk, silica, sol-gel, drug carrier, α-mangostin

## 1. INTRODUCTION

Drug delivery system is based on the interdisciplinary approach that combines polymer science, bioconjugate chemistry, pharmaceutics and molecular biology.[1] It is a component of formulation or a device that promotes therapeutic substance in the body and improves its efficacy and safety by controlling the rate, time and

place of the drug release with a therapeutic concentration. In drug delivery system, drug carrier transports, retains and delivers the drug within or in the vicinity of the target.[2] Most of the currently used carriers are either natural or synthetic polymers such as microcapsules, cells, lipoproteins, etc. Besides that, there are also increasing number of studies on alternative supports such as silica-based materials.

Mangosteen (*Garcinia mangostana*) is a fruit originated from Southeast Asia. Also known as the "queen" of all fruits, it contains a high amount of α-mangostin ($C_{24}H_{26}O_6$). The compound demonstrates properties of antioxidant, antibacterial, antifungal, anti-inflammatory, anticancer, antituberculosis activities and it is also being used as a mosquito larvicide.[3] Though beneficial to human health, α-mangostin has poor solubility and low oral bioavailability. In order to enhance its solubility and dissolution, Sodalee et al. adsorbed the α-mangostin containing liquid SEDDS (a mixture of water, oil, surfactant and co-surfactant) onto two different types of silica (Aeropel 300 and Sylysia 350).[4] It was found that the solubility and dissolution of α-mangostin adsorbed on Aeropel 300 were better than Sylysia 350.

Rice husk ash (RHA) obtained from incinerating rice husk (RH) under controlled environment produces amorphous silica. The purity of the amorphous silica in RHA is ca. 92%–95%, which can be further purified to 99.9%.[5] RHA exhibits high reactivity, large surface area and a superfine size. The RHA silica modified with metals and organic compounds have been successfully used as heterogeneous catalysts in various catalytic processes.[6–8] However, no reports can be found on the use of RHA silica as a drug carrier. This prompted an investigation on the feasibility of RHA silica as a drug carrier for α-mangostin and herein we report our findings.

## 2. EXPERIMENTAL

### 2.1 Chemicals and Raw Materials

The chemicals used were hydrochloric acid (Systerm, Shah Alam, Selangor, Malaysia, 37%), sodium hydroxide pellets (Systerm, 99%), nitric acid (Systerm, 65%), 1,3,5 trimethylbenzene (Sigma Aldrich, Buchs, Switzerland), Pluronic P-123 (Sigma Aldrich), α-mangostin (Sigma Aldrich), Tween 80 (Sigma Aldrich), acetonitrile (Sigma Aldrich, HPLC grade), absolute ethanol (Sigma Aldrich) and acetic acid (Systerm, 99.5%). All chemicals were used as received without further purification. RH was collected from a rice mill in Temerloh, Pahang, Malaysia.

## 2.2 Characterisations

The surface morphology of the samples were determined at 15 kV using a JSM-6390 field emission-scanning electron microscope (FESEM) from JEOL (Tokyo, Japan). The FTIR spectrum was obtained using KBr pellet method on a 1600 Series Perkin Elmer spectrophotometer (Massachusetts, US) in the range of 400–4000 $cm^{-1}$. Thermogravimetric analysis was performed with Perkin-Elmer thermogravimetric analyser (TGA 7) at a heating rate of 10°C $min^{-1}$ under a nitrogen atmosphere from room temperature to 850°C. The $N_2$ adsorption analysis was carried out using a porosimeter (model NOVA Quantachrome porosimeter 2000e) at 77 K. Adsorption branch was used to determine the BJH pore size distribution.

## 2.3 Preparation of Sodium Silicate Solution

The RHA was prepared according to the method reported by Adam et al.[9] The RH was washed with tap water several times to remove dirt and then dried for 48 h at room temperature. The metallic impurities in the RH was removed by stirring the RH (30 g) in 750 ml of 1.0 M nitric acid for 24 h in a plastic container. The acid treated RH was filtered and rinsed with distilled water until the pH of the filtrate became constant. The acid treated RH was then dried at 110°C for 24 h before calcination at 600°C for 6 h to obtain RHA. Sodium silicate from RHA was prepared by dissolving 30 g of RHA in 300 ml of 1 M NaOH.

## 2.4 Synthesis of Mesoporous Silica (RHA-Si)

The RHA-Si was synthesised using Pluronic 123 as a structure-directing agent and 1,3,5-trimethylbenzene (TMB) as micelle expander. The Pluronic 123 (3 g) and TMB (2.5 ml) were added into the sodium silicate solution and stirred until the solution became homogeneous. Hydrochloric acid (1 M) was added into the solution to reduce the pH to 9. Subsequently, the solution was stirred for 20 h at 35°C. The solution was then aged at 100°C for 48 h without stirring. The gel was centrifuged and dried at 100°C for 24 h followed by calcination at 600°C for 6 h to remove the surfactant and the pore expander. The resulting gel was ground into fine powder.

## 2.5 Adsorption of α-Mangostin on RHA-Si

The α-mangostin (3 mg) was dissolved in 5 ml of ethanol. Into the solution, 50 mg of RHA-Si was added. The mixture was stirred at 35°C to remove the ethanol. The sample was dried for 24 h at 100°C. RHA-Si loaded with α-mangostin was labeled as RHA-Si-α.

### 2.6 In-vitro Release Test

The in-vitro release test was conducted according to the method described by Ali et al.[10] RHA-Si-α (53 mg) was suspended in 1 ml PBS (pH 7.4) containing 2000 µl of 0.1% Tween 80 in an Eppendorf tube. The tube was placed vertically without agitation at 37°C for one week. At pre-determined time intervals (15 min, 30 min, 1 h, 3 h, 24 h and 168 h), aliquots were withdrawn and centrifuged at 300 rpm for 3 min. The volume of supernatant withdrawn was replenished with an equal volume of fresh medium. The supernatant consisting of α-mangostin was diluted with 70% v/v acetonitrile, filtered through 0.2 µm PTFE microfilter and immediately analysed by HPLC.

### 2.7 Chromatographic Conditions

The quantity of α-mangostin released from the carrier was determined using HPLC at ambient temperature. The quantification wavelength of α-mangostin was set at 250 nm. The HPLC system (Agilent, series 1100, US) was equipped with a C-18 guard column (Supelco sigma-Aldrich; 15 cm × 4.6 mm, 5 µm), quaternary pump (G1311A), autosampler (G1313A), solvent degasser (G1379A) and UV detector (G1314B). The mobile phase consisted of acetonitrile and 0.1% (v/v) acetic acid diluted in water. The mobile phase solutions were freshly prepared, filtered through 0.45 µm Nylon filter and degassed by sonication for 15 min prior to use. The sample injection volume was adjusted to 10 µl. ChemStation software was used to analyse the results.

### 2.8 Preparation of Calibration Curve

A stock solution with final concentration of 1 mg $ml^{-1}$ was prepared by dissolving an accurately weighed α-mangostin in a mixture of acetonitrile and PBS (70:30, v/v). Standard solutions of 1 µg $ml^{-1}$, 2 µg $ml^{-1}$, 4 µg $ml^{-1}$, 6 µg $ml^{-1}$, 8 µg $ml^{-1}$, 10 µg $ml^{-1}$, 20 µg $ml^{-1}$, 40 µg $ml^{-1}$, 60 µg $ml^{-1}$, 80 µg $ml^{-1}$, 100 µg $ml^{-1}$ and 200 µg $ml^{-1}$ were prepared by serial dilution of the stock solution. The standard solutions were injected in triplicate and the linearity was assessed based on the calibration equation calculated from plotting the mean peak areas versus corresponding concentrations.

## 3. RESULTS AND DISCUSSION

### 3.1 FTIR Spectroscopic Analysis

The FTIR spectrum of RHA-Si is shown in Figure 1(a). The broad band at 3441 $cm^{-1}$ was assigned to O-H vibration from Si-OH and $H_2O$ adsorbed on the

surface of silica. The band around 1633 $cm^{-1}$ was assigned to the HO-H bending vibration of $H_2O$ trapped within the silica matrix. An asymmetric stretching vibration of the structural siloxane bond (Si-O-Si) was indicated by a strong band at 1099 $cm^{-1}$. The bands at 805 $cm^{-1}$ and 471 $cm^{-1}$ were attributed to the symmetric stretching and bending mode of the bulk Si-O-Si bond. The band at 960 $cm^{-1}$ was attributed to Si-OH stretching vibration of the surface silanol groups.[11,12]

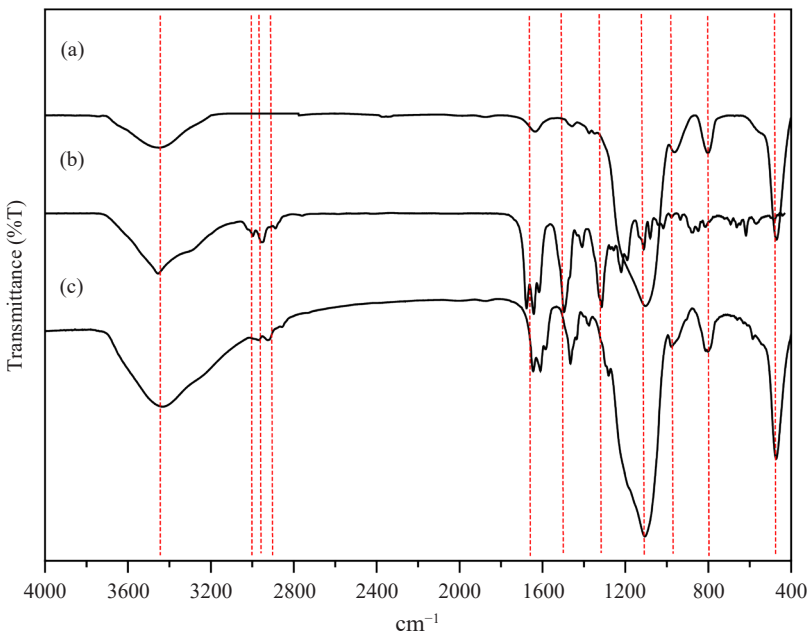


Figure 1: The FTIR spectra of (a) RHA-Si, (b) α-mangostin and (c) RHA-Si-α.

The FTIR spectrum of α-mangostin is shown in Figure 1(b). The vibrational stretching band of O-H appears at 3424 $cm^{-1}$ whereas the vibrational stretching of C=O appears at 1648 $cm^{-1}$. The band at 1463 $cm^{-1}$ showed the presence of aromatic C=C stretching vibration while the band at 1100 $cm^{-1}$ is due to the C-O stretching of the ether bond. The stretching bands at 2854 $cm^{-1}$, 2919 $cm^{-1}$ and 2965 $cm^{-1}$ were assigned to the C-H vibration of the methyl groups of α-mangostin.[3]

Figure 1(c) indicates the FTIR spectrum of RHA-Si-α. From the spectrum, stretching bands related to the C-H vibration of the methyl groups α-mangostin can be seen between 3000 $cm^{-1}$ and 2600 $cm^{-1}$. The bands between 1800 $cm^{-1}$ and 1000 $cm^{-1}$ can be assigned to the vibrational stretching of C=O groups (1648 $cm^{-1}$), aromatic C=C groups (1463 $cm^{-1}$) and C-O ether groups (1100 $cm^{-1}$) of α-mangostin. The bands related exclusively to the symmetric stretching and bending modes of bulk Si-O-Si bond can be seen between 805 $cm^{-1}$ and 471 $cm^{-1}$. The strong band at 1099 $cm^{-1}$ was due to the asymmetric stretching vibration of the structural

siloxane bond (Si-O-Si). The co-existence of bands related to functional groups of silica and α-mangostin indicate that α-mangostin has been successfully adsorbed on the surface of RHA-Si-α.

The silanol groups that exist on the surface of any siliceous materials can be categorised as isolated, vicinal or germinal depending on the degree of condensation of silanol to siloxane linkages, Si-O-Si. The α-mangostin is suggested to initially form hydrogen bonds with the silanol groups as shown in Scheme 1. The subsequent adsorption of α-mangostin leading towards the formation of multilayer is considered to take place via physical adsorption.

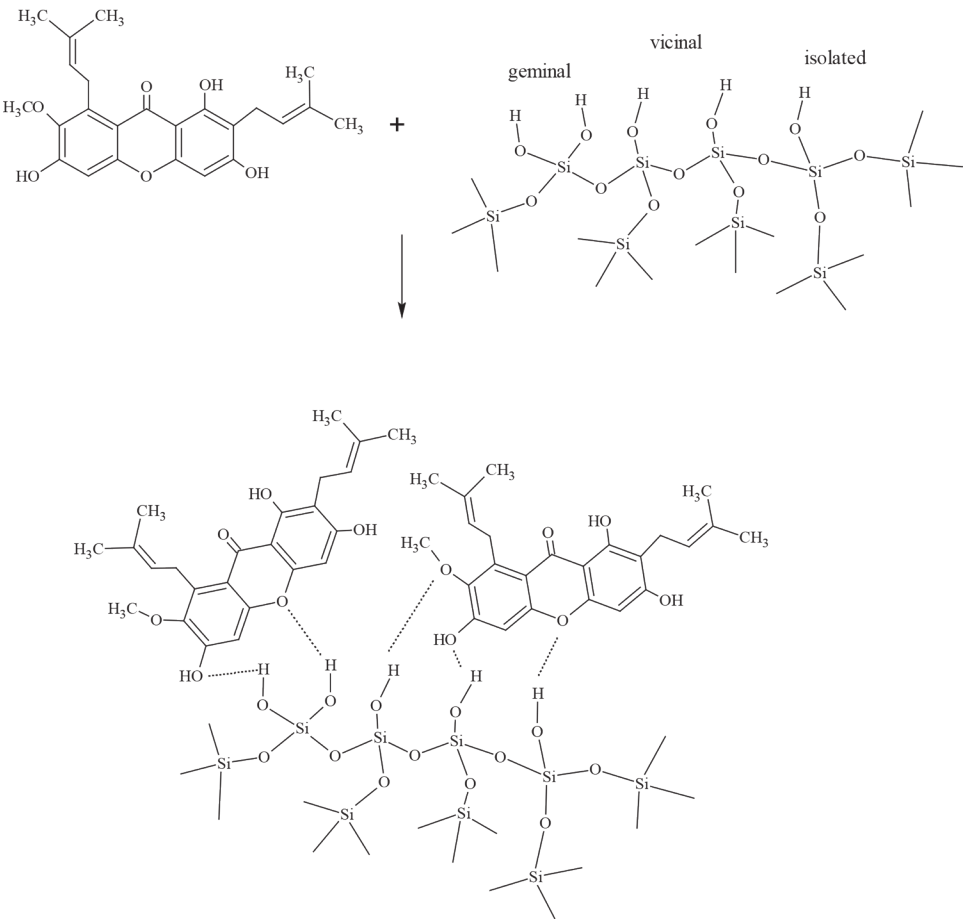


Scheme 1: The possible hydrogen bond (shown in dotted lines) interaction between the germinal, vicinal and isolated surface silanol groups of RHA-Si and α-mangostin.

### 3.2 Nitrogen Adsorption-desorption Analysis

The nitrogen adsorption-desorption isotherms of RHA-Si and RHA-Si-α are shown in Figure 2. Based on the isotherm, RHA-Si exhibits a combination of type I and type IV isotherms with H2 hysteresis loop, as in Figure 2(a). The type I isotherm can be seen by the appearance of "knee" at a low relative pressure whereas the type IV isotherm characteristic can be seen from the presence of hysteresis loop around relative pressure 0.42. These are the indications that RHA-Si contains mostly mesopores with a small percent of micropores according to IUPAC.[13] The BJH pore size was determined to be 5.1 nm.

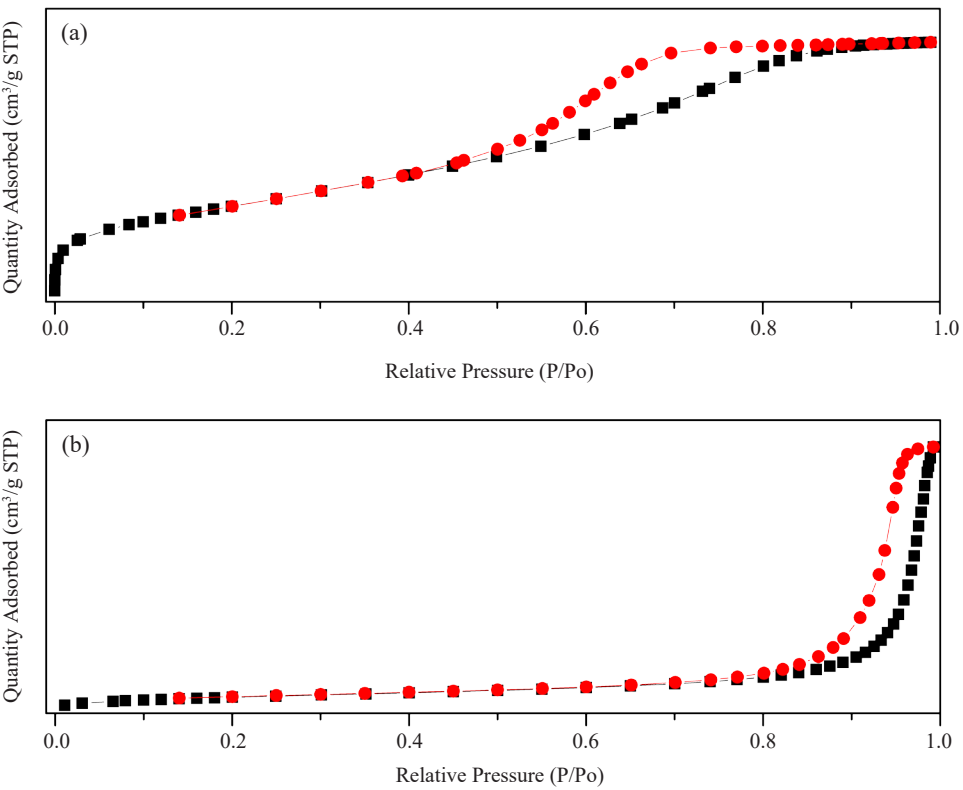


Figure 2: The $N_2$ adsorption-desorption isotherm of (a) RHA-Si (b) RHA-Si-α.

RHA-Si-α exhibits type IV isotherm with H3 hysteresis loop, as in Figure 2(b). The disappearance of the knee at the lower relative pressure and the hysteresis loop at higher relative pressure indicate that RHA-Si-α contains larger pore system compared to the RHA-Si. The pore size was found to be 24.4 nm. The BET surface area was reduced from 589 $m^2g^{-1}$ to 110 $m^2g^{-1}$. The disappearance of knee, shifting of hysteresis loop and increase in the pore size suggest that α-mangostin

may have closed all the smaller pores of RHA-Si and started to aggregate on the surface forming new pore systems with a larger diameter. The H3 hysteresis loop indicates non-rigid aggregation of plate-like particles giving rise to slit-shaped pores. The pore volume of RHA-Si-α (0.67 $cm^3$ $g^{-1}$) is lower compared to the RHA-Si (0.75 $cm^3$ $g^{-1}$) which is in agreement with the variation in their specific surface area. The nitrogen adsorption-desorption data of RHA-Si and RHA- Si-α are summarised in Table 1.

Table 1: The $N_2$ adsorption-desorption data of RHA-Si and RHA-Si-α determined at 77 K.

| | Hysteresis loop | Surface area ($m^2$ $g^{-1}$) | Pore volume ($cm^3$ $g^{-1}$) | Pore size (nm) |
|---|---|---|---|---|
| RHA-Si | H2 | 589 | 0.75 | 5.1 |
| RHA-Si-α | H3 | 110 | 0.67 | 24.4 |

## 3.3 FESEM Microscopic Analysis

The FESEM images of RHA-Si and RHA-Si-α are shown in Figure 3. The surface of RHA-Si contains voids (shown with white arrows) in between chunky particles whereas fewer and smaller voids can be seen on the surface of RHA-Si-α. The particles on the surface of RHA-Si-α have a plate-like morphology.

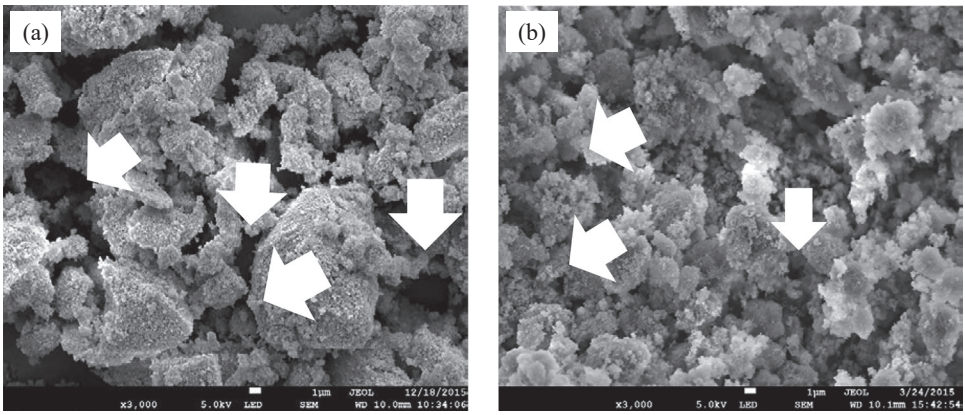


Figure 3: The FESEM images of (a) RHA-Si and (b) RHA-Si-α. The voids (shown in white arrows) are more prominent and bigger in RHA-Si compared to RHA-α.

## 3.4 TGA

The TGA thermograms of RHA-Si, RHA-Si-α and α-mangostin, are shown in Figure 4. Based on Figures 4(a) and 4(b), weight loss that occurred before 200°C

was due to physically adsorbed water molecules. The weight loss of adsorbed water molecules for RHA-Si was *ca.* 3.97% (0.1434 mg) whereas for RHA-Si-α, the weight loss was *ca.* 3.46% (0.1867 mg). The remaining weight loss (*ca.* 2.19%, 0.07908 mg) at 200°C−550°C for RHA-Si was due to the condensation of silanol groups to form siloxane bonds. Above 600°C, the weight gain observed could be due to the reaction of $N_2$ on the surface of RHA-Si. From the thermogram of α-mangostin, shown Figure 4(c), the initial weight loss (*ca.* 0.18%, 0.004 mg) was due to the moisture followed by a sharp endothermic peak at 260°C which was attributed to the burning off of the organic into $CO_2$ (*ca.* 85.4%, 1.915 mg). At higher temperature, further weight loss (*ca.* 5.6%, 0.1267 mg) was attributed to the decomposition of remaining organic groups. For RHA-Si-α (Figure 4(b)), the weight loss (ca. 32.3%, 1.740 mg) around 200°C−550°C can be attributed to the decomposition of α-mangostin attached to the inorganic silica backbone and the condensation of silanol groups to siloxane groups.[14] The TGA provided further evidence for the successful immobilisation of α-mangostin on the RHA-Si.

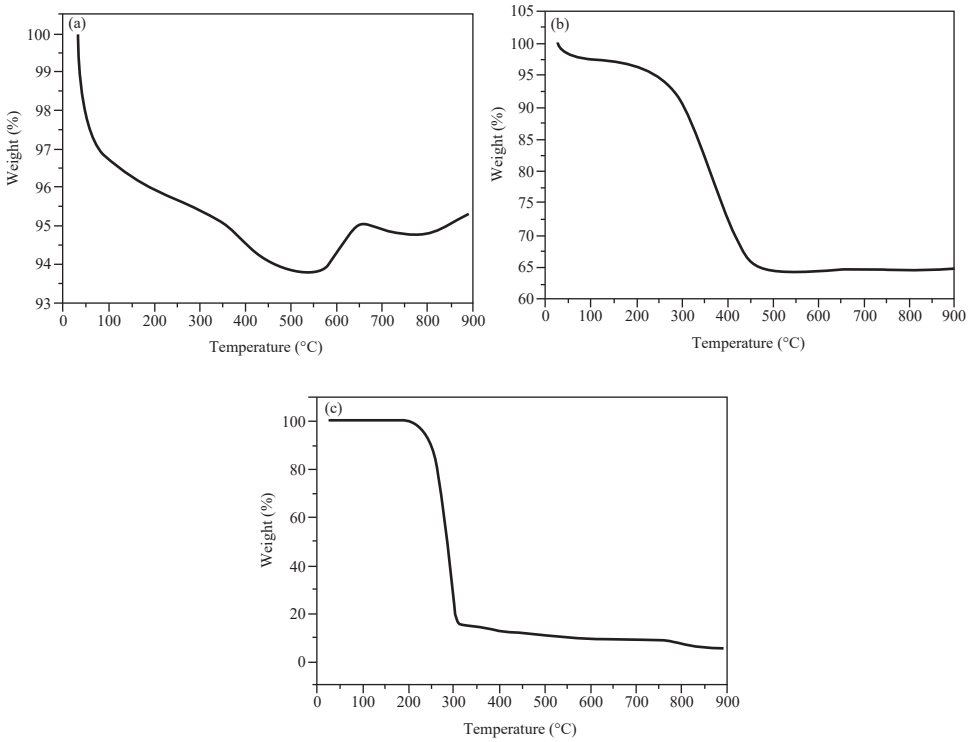


Figure 4: The thermogravimetric analysis of (a) RHA-Si, (b) RHA-Si-α and (c) α-mangostin.

### 3.5 XRD Analysis

The XRD diffractograms of RHA-Si, α-mangostin and RHA-Si-α are shown in Figure 5. Only a broad peak at 2θ = 22° can be observed in the diffractogram of RHA-Si, shown in Figure 5(a) and RHA-Si-α, as in Figure 5(b). This broad peak is associated with the amorphous nature of the silica.[15] The interaction between the silanol groups of RHA-Si with the α-mangostin may have disrupted the crystal lattice of the drug. The disruption had prevented the drug from retaining its crystallinity when adsorbed on the surface. The disappearance of the crystallinity indicates that the solubility and bioavailability of the drug have been increased. Any drugs in its crystalline state tend to have poor solubility and dissolution since higher energy is required to break the crystal lattice.

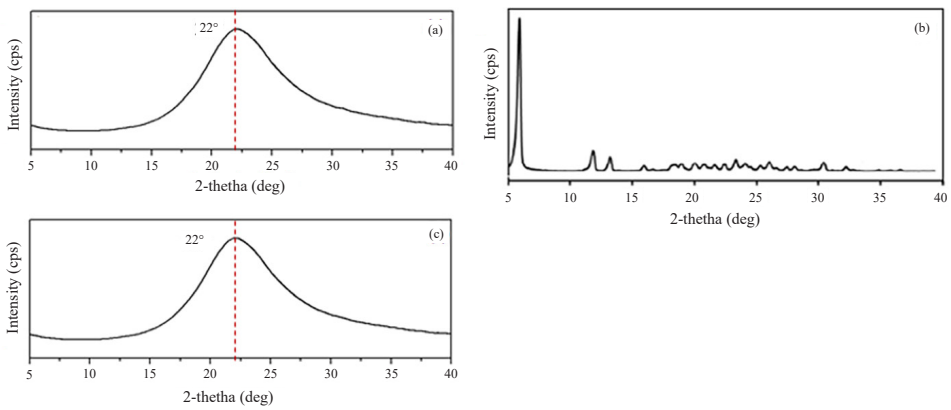


Figure 5: The XRD diffractograms of (a) RHA-Si, (b) α-mangostin and (c) RHA-Si-α.[16]

### 3.6 In-vitro Release Test

The mean percentage of cumulative release of α-mangostin is shown in Table 2. In this study, Tween 80 solution was used as it has the ability to reduce the interfacial tension of the α-mangostin particle. This condition allowed the expected amount of the drug to dissolve or to encounter the "sink condition" during the drug release.[10] As shown in Table 2, the first stage was initiated with the burst release corresponding to 47% of the total drug loading in the first 15 min. Then, the drug sustained in slow drug release. The interaction between physically adsorbed α-mangostin and silica are weaker compared to those that are chemically bonded. The burst release must be due to the release of the physically adsorbed α-mangostin. Subsequent release required longer time because of stronger interaction between the drug molecules and the surface of the silica. The burst release suggested that the solubility and dissolution of α-mangostin have been enhanced. This is in line with finding from the XRD analysis.

Table 2: The mean percentage of cumulative release of α-mangostin.

| Time | Cumulative release (%) |
|---|---|
| 15 min | 47.02 ± 8.3 |
| 30 min | 47.15 ± 7.1 |
| 1 h | 47.37 ± 6.9 |
| 3 h | 47.69 ± 6.9 |
| 24 h | 47.84 ± 6.8 |
| 168 h | 48.23 ± 6.3 |

*Notes: Concentration = 600 ug ml; *Percentage of α-mangostin drug release = (X/concentration*100)*

## 4. CONCLUSION

RHA-Si was prepared from RHA as a potential carrier for α-mangostin. Physicochemical characterisations indicate successful adsorption of α-mangostin on the surface of RHA-Si. The drug release test showed burst release effect corresponding to 47% of the total drug loading in first 15 min. The burst release indicates that the solubility and bioavailability of α-mangostin have increased upon the adsorption on the carrier. The characterisations in vitro release test results suggest that RHA silica has a huge potential to be developed and used in pain management which requires immediate release of drugs.

## 5. ACKNOWLEDGEMENTS

The authors are grateful to the Ministry of Higher Education (MOHE) Malaysia for financial support (FRGS-13-035-0276) and Universiti Sains Malaysia Short Term Grant (1001/PKIMIA/6313215).

## 6. REFERENCES

1. Devi, V. K., Jain, N. & Valli, K. S. (2001). Importance of novel drug delivery systems in herbal medicines. *Pharm. Rev.*, 4, 27–31, http://doi.org/10.4103/0973-7847.65322.
2. Tiwari, G. et al. (2012). Drug delivery systems: An updated review. *Int. J. Pharm. Invest.*, 2, 2–11, http://doi.org/10.4103/2230-973X.96920.
3. Ahmad, M., Yamin, B. M. & Lazim, A. M. (2013). A study on dispersion and characterisation of α-mangostin loaded pH sensitive microgel systems. *Chem Cen. J.*, 7, 85, https://doi.org/10.1186/1752-153X-7-85.

4. Sodalee, K. et al. (2016). Preparation and evaluation of alpha-mangostin solid self-emulsifying drug delivery system. *Asian J. Pharm.*, 11, 225−226, https://doi.org/10.1016/j.ajps.2015.11.024.
5. Radhika, T. & Sungunan, S. (2006). Structural and catalytic investigation of Vanadia supported on ceria promoted with high surface area rice husk silica. *J. Mol. Catal. A Chem.*, 250, 169−176, https://doi.org/10.1016/j.molcata.2006.01.048.
6. Adam F. & Kueh, C. (2015). Heterogeneous para-phenylamino sulfonic acid ligand functionalized on MCM-41 derived from rice husk ash: Selective mono-alkylated products of tert-butylation of phenol. *Appl. Catal. A Gen.*, 489, 162−170, https://doi.org/10.1016/j.apcata.2014.09.047.
7. Adam, F. & Iqbal, A. (2011). The liquid phase oxidation of styrene with tungsten modified silica as a catalyst. *Chem. Eng. J.*, 171, 1379–1386, https://doi.org/10.1016/j.cej.2011.05.052.
8. Adam, F., Hello, K. M. & Aisha, M. R. B. (2011). The synthesis of heterogeneous 7-amino-1-naphthalene sulfonic acid immobilized silica nano particles and its catalytic activity. *J. Taiwan Inst. Chem. Eng.*, 42, 843−851, https://doi.org/10.1016/j.jtice.2011.02.002.
9. Adam, F., Balakrishnan, S. & Wong, P. L. (2006). Rice husk ash silica as a new support material for ruthenium based heterogenous catalyst. *J. Phys. Sci.*, 17(2), 1−13.
10. Ali, A. A. E., Taher, M. & Mohamed, F. (2013). Microencapsulation of alpha-mangostin into PLGA microspheres and optimization using response surface methodology intended for pulmonary delivery. *J. Microenc.*, 30(8), 728−740, https://doi.org/10.3109/02652048.2013.788081.
11. Cruz, R. S. D. et al. (2001). Catalytic activity and stability of chromium containing silicate in liquid phase cyclohexane oxidation. *J. Mol. Catal. A Chem.*, 171(1), 258−267, https://doi.org/10.1016/S1381-1169 (01)00111-X.
12. Parida, S. K. et al. (2006). Adsorption of organic molecules on silica surface. *Adv. Colloid Interf. Sci.*, 121, 77−110, https://doi.org/10.1016/j.cis.2006.05.028.
13. Lowell, S. et al. (2004). *Characterization of porous solids and powders: surface area, pore size and pore density*. Amsterdam: Kluwer Academic Publishers.
14. Magar, R. L. et al. (2013). Silica gel supported polyamine: A versatile catalyst for one pot synthesis of 2-amino-4H-chromene derivatives. *J. Mol. Catal. A Chem.*, 374–375:118–124, https://doi.org/10.1016/j.molcata.2013.03.022.

15. Adam, F., Chew, T. S. & Andas, J. (2011). A simple template-free sol-gel synthesis of spherical nanosilica from agricultural biomass. *J. Sol-Gel. Sci. Technol*., 59(3), 580–583, https://doi.org/10.1007/s10971-011-2531-7.
16. Samprasit, W. et al. (2015). Fabrication and in vitro / in vivo performance of mucoadhesive electrospun nanofiber mats containing α-mangostin. *AAPS PharmSciTech.*, 16(5), 1140−1152, https://doi.org/10.1208/s12249-015-0300-6.